(10 to 70 Tg/year) and top-down (140 to 910 Tg/year) estimates of global SOA production (*30*). Nevertheless, IEPOX is expected to undergo hundreds of collisions with aerosol surfaces before reacting with OH, and its detection in the atmosphere (fig. S8) suggests that a complex suite of conditions likely controls its uptake to aerosols (e.g., the pH and chemical composition of aerosol). Furthermore, *i*SOA formation may depend on the unquantified differences in the yields and uptake characteristics of the β- and δ-IEPOX. Quantitative understanding of these complex interactions is required to assess the effect of this chemistry on the overall SOA abundance and its associated impacts [e.g., cloud condensation nuclei (*31*)].

The efficient formation of dihydroxyepoxides, a previously unknown class of gas-phase compounds, addresses many of the issues currently being debated about isoprene chemistry. Because their formation is accompanied by the reformation of OH, this chemistry contributes to the remarkable stability of HO_x in remote regions of the troposphere subjected to high isoprene emissions. The formation of IEPOX also provides a gas-phase precursor for the *i*SOA formation. Further investigation of the multiphase chemistry of IEPOX is needed to elucidate the complex interaction between emissions from the biosphere and atmospheric composition (*32*, *33*). In particular, the development of a proper chemical description of these interactions is essential for assessing the sensitivity of this chemistry to changes in isoprene emissions caused by environmental changes (e.g., climate change and deforestation) and to the further development of anthropogenic activities and the accompanying NO_x emissions in these regions.

References and Notes

1. A. Guenther *et al.*, *Atmos. Chem. Phys.* **6**, 3181 (2006).
2. P. C. Harley, R. K. Monson, M. T. Lerdau, *Oecologia* **118**, 109 (1999).
3. J. D. Fuentes *et al.*, *Bull. Am. Meteorol. Soc.* **81**, 1537 (2000).
4. T. N. Rosenstiel, M. J. Potosnak, K. L. Griffin, R. Fall, R. K. Monson, *Nature* **421**, 256 (2003).
5. C. Wiedinmyer, X. Tie, A. Guenther, R. Neilson, C. Granier, *Earth Interact.* **10**, 1 (2006).
6. R. von Kuhlmann, M. G. Lawrence, U. Pöschl, P. J. Crutzen, *Atmos. Chem. Phys.* **4**, 1 (2004).
7. M. Claeys *et al.*, *Science* **303**, 1173 (2004).
8. P. Crutzen *et al.*, *Atmos. Environ.* **34**, 1161 (2000).
9. C. E. Reeves, S. A. Penkett, *Chem. Rev.* **103**, 5199 (2003).
10. J. A. Thornton *et al.*, *J. Geophys. Res.* **107**, 17 (2002).
11. J. Lelieveld *et al.*, *Nature* **452**, 737 (2008).
12. X. Ren *et al.*, *J. Geophys. Res.* **113**, 5310 (2008).
13. Materials and methods are available as supporting material on *Science* Online.
14. J. Peeters, T. L. Nguyen, L. Vereecken, *Phys. Chem. Chem. Phys.*, **11**, 5935 (2009).
15. T. J. Dillon, J. N. Crowley, *Atmos. Chem. Phys.* **8**, 4877 (2008).
16. E. R. Bell, F. F. Rust, W. E. Vaughan, *J. Am. Chem. Soc.* **72**, 337 (1950).
17. W. Wang *et al.*, *Rapid Commun. Mass Spectrom.* **19**, 1343 (2005).
18. J. D. Surratt *et al.*, *J. Phys. Chem. A* **110**, 9665 (2006).
19. E. C. Minerath, M. J. Elrod, *Environ. Sci. Technol.* **43**, 1386 (2009).
20. J. D. Crounse, K. A. McKinney, A. J. Kwan, P. O. Wennberg, *Anal. Chem.* **78**, 6726 (2006).
21. F. Paulot *et al.*, *Atmos. Chem. Phys.* **9**, 1479 (2009).
22. F. W. McLafferty, *Science* **214**, 280 (1981).
23. L. Ruppert, K. H. Becker, *Atmos. Environ.* **34**, 1529 (2000).
24. J. D. Surratt *et al.*, *J. Phys. Chem. A* **112**, 8345 (2008).
25. S. Gao *et al.*, *Environ. Sci. Technol.* **38**, 6582 (2004).
26. I. Bey *et al.*, *J. Geophys. Res.* **106**, 73 (2001).
27. J. D. Surratt *et al.*, *Environ. Sci. Technol.* **41**, 5363 (2007).
28. J. A. de Gouw *et al.*, *J. Geophys. Res.* **110**, D16305 (2005).
29. P. Tunved *et al.*, *Science* **312**, 261 (2006).
30. A. H. Goldstein, I. E. Galbally, *Environ. Sci. Technol.* **41**, 1515 (2007).
31. V.-M. Kerminen, H. Lihavainen, M. Komppula, Y. Viisanen, M. Kulmala, *Geophys. Res. Lett.* **32**, L14803 (2005).
32. F. W. Went, *Nature* **187**, 641 (1960).
33. M. O. Andreae, P. J. Crutzen, *Science* **276**, 1052 (1997).

34. We thank X. Levine, H. O. T. Pye, and the Harvard GEOS CHEM team (Daniel J. Jacob, principal investigator) for their help in setting up the GEOS-CHEM model; A. J. Kwan, A. W. Chan, P. S. Chhabra, and N. Eddingsaas for experimental assistance; J. D. Surratt for providing the speciation of the SOA resulting from BEPOX reactive uptake; and J. Lane, I. Maxwell-Cameron, and S. Jørgensen for helpful discussions regarding the quantum calculations. F.P. was partially supported by the William and Sonya Davidow fellowship. J.D.C. thanks the EPA Science to Achieve Results (STAR) Fellowship Program (FP916334012) for providing partial support. The mass spectrometer used in this study was purchased as part of a major research instrumentation grant from the National Science Foundation (ATM-0619783). Assembly and testing of the CIMS instrument was supported by the Davidow Discovery Fund. The numerical simulations for this research were performed on Caltech's Division of Geological and Planetary Sciences Dell Cluster. This work was supported by the Office of Science (Biological and Environmental Research), U.S. Department of Energy grant DE-FG02-05ER63983, U.S. Environmental Protection Agency STAR agreement RD-833749, and the Marsden Fund administrated by the Royal Society of New Zealand. The TC4 and ARCTAS campaigns were supported by NASA grants NNX07AL33G and NNX08AD29G. This work has not been formally reviewed by the EPA. The views expressed in this document are solely those of the authors, and the EPA does not endorse any products or commercial services mentioned in this publication.

Supporting Online Material

www.sciencemag.org/cgi/content/full/325/5941/730/DC1
Materials and Methods
Figs. S1 to S9
Tables S1 to S9
References

2 March 2009; accepted 24 June 2009
10.1126/science.1172910

Phylogenetic Conservatism of Extinctions in Marine Bivalves

Kaustuv Roy,[1]* Gene Hunt,[2] David Jablonski[3]

Evolutionary histories of species and lineages can influence their vulnerabilities to extinction, but the importance of this effect remains poorly explored for extinctions in the geologic past. When analyzed using a standardized taxonomy within a phylogenetic framework, extinction rates of marine bivalves estimated from the fossil record for the last ~200 million years show conservatism at multiple levels of evolutionary divergence, both within individual families and among related families. The strength of such phylogenetic clustering varies over time and is influenced by earlier extinction history, especially by the demise of volatile taxa in the end-Cretaceous mass extinction. Analyses of the evolutionary roles of ancient extinctions and predictive models of vulnerability of taxa to future natural and anthropogenic stressors should take phylogenetic relationships and extinction history into account.

Groups of organisms differ in their vulnerability to extinction (*1*–*5*), but the nature and magnitude of that variation is still poorly quantified. Extinction risk of species and lineages is determined by a variety of ecological and life history traits (*2*), as well as emergent properties such as geographic range (*5*–*8*). Many of these extinction-related traits are phylogenetically conserved, suggesting that extinctions should be phylogenetically clustered: Taxa in some clades should be consistently more extinction-prone than others (*3*, *9*, *10*). Consistent with this idea, current extinction risk and documented anthropogenic extinctions are nonrandomly distributed among vertebrate lineages (*9*, *11*–*15*), but whether such phylogenetic selectivity holds in general, including for extinctions in the geologic past, remains poorly known. In this study, we used the Mesozoic-Cenozoic fossil record of marine bivalves, in conjunction with molecular phylogenies, to test for phylogenetic clustering of extinctions within and among bivalve families and how this clustering varies over time.

The fossil record of marine bivalves preserves a rich history of past extinctions, and although this record is not free of taphonomic biases, such biases are increasingly well understood (*16*, *17*). We used a taxonomically standardized database

[1]Section of Ecology, Behavior and Evolution, University of California San Diego, La Jolla, CA 92093–0116, USA. [2]Department of Paleobiology, National Museum of Natural History, Smithsonian Institution, Washington, DC 20013–7012, USA. [3]Department of Geophysical Sciences, University of Chicago, 5734 South Ellis Avenue, Chicago, IL 60637, USA.

*To whom correspondence should be addressed. E-mail: kroy@ucsd.edu

of stratigraphic ranges of marine bivalves (*18*) to calculate background extinction rates (i.e., for times other than the massive end-Cretaceous event) of 1678 genera and subgenera (hereafter termed genera) over the last ~200 million years (Jurassic to Pleistocene). Genera are the preferred units of large-scale paleontological analyses because, relative to species, their taxonomy is better standardized and more stable, and their fossil record is far more complete and more robust to taphonomic biases (*19*, *20*). Furthermore, comparative analyses indicate that morphologically defined molluscan genera generally reflect the topologies of molecular phylogenies (*21*). Taxonomic standardization is clearly a prerequisite for any quantitative analysis of extinction rates, and the data we used were subjected to extensive revisions and standardization (*18*, *19*, *22*). We used the family level for analyses of phylogenetic clustering of extinction rates because families provide the necessary balance between adequate sample size and phylogenetic resolution. In general, families of marine bivalves have proven to be robust taxonomic units, and recent molecular phylogenies suggest that none of the major families of marine bivalves are blatantly polyphyletic (*23*). Although some bivalve families may prove to be paraphyletic when a more complete molecular phylogeny of the group is available, for our analyses, paraphyly is more likely to add noise than to produce artifactual trends.

If extinctions of bivalve genera were random with respect to family membership, then an index of taxonomic clustering for individual extinction events [R_{CL} (*18*)] should not differ systematically from zero across a time series of such events. Positive values of R_{CL} indicate more (and negative values less) clustering than random extinction (*18*). Of the 26 standard time intervals in our data (*18*) for which R_{CL} could be reliably calculated, 21 (81%) have positive values (Fig. 1), a result that is highly unlikely under a model of phylogenetically random extinctions ($P = 0.002$, exact binomial test). When R_{CL} for individual time intervals is compared with the null distribution for that interval (*18*), 8 out of the 26 intervals show significantly positive clustering (i.e., the observed R_{CL} is at least as great as the upper 95% confidence limit), and no interval is significantly less clustered than random (Fig. 1). These eight intervals include the end-Cretaceous event, the only major mass extinction in our data. A ninth interval, the Campanian, is marginally significant. Thus extinctions of marine bivalves over the last 200 million years show a general pattern of phylogenetic conservatism within families, both during background and mass extinctions, but the strength of such clustering varies over time, and not all extinctions show significant clustering.

Our data also reveal that extinction magnitude is not correlated with phylogenetic clustering. The highest R_{CL} value is associated with the end-Cretaceous mass extinction (Fig. 2), but many high-extinction intervals, such as the Late Eocene, lack strong clustering (table S1), and the overall relation between phylogenetic clustering and extinction intensity is not significant (Spearman rank correlation, $r_s = 0.20$, $P = 0.34$). Extinction rates declined significantly over time, but this decline was caused by culling of volatile clades rather than by a decrease in extinction intensity within individual clades. Overall, rates before the end-Cretaceous extinction (excluding the Maastrichtian stage, which ends with the mass extinction) are higher than in the Cenozoic (median for Mesozoic stages = 0.087, median for Cenozoic stages = 0.029; Wilcoxon rank sum test, $W = 157$, $P = 0.054$). For families well-represented in both the Mesozoic and the Cenozoic, extinction rates do not differ significantly before and after the end-Cretaceous event (Wilcoxon paired signed rank test, $V = 61$, $P = 0.74$, $n = 16$ families), and families show high rank-order agreement between Mesozoic and Cenozoic background rates of extinction (Fig. 3) (Spearman rank correlation, $r_s = 0.75$, $P = 0.0008$). The lower Cenozoic extinction rates instead result from preferential losses during the end-Cretaceous extinction in families with inherently high extinction rates (Fig. 4), so that Cenozoic bivalve diversity was dominated by the more extinction-resistant families. The three families with the highest Mesozoic background extinction rates went globally extinct at the end of the Cretaceous, and other high-rate Mesozoic clades (e.g., trigoniids and arcticids, both with background rates >0.15, at least twice the Mesozoic median) (Fig. 4) were severely hit and have since remained minor components of the bivalve fauna. The only family for which background extinction rates were much lower in the Cenozoic than the Mesozoic is the Veneridae, which also suffered major losses at the end of the Cretaceous. Thus, the end-Cretaceous extinction had a filtering effect on lineage-specific extinction rates, removing the most volatile families but not systematically altering within-family extinction rates.

Extinction rates analyzed in conjunction with recently published molecular phylogenies of living bivalve families (*18*) also indicate phylogenetic conservatism at deeper levels in the bivalve tree. Extinction rates of closely related families are significantly more similar to each other than is expected by chance (Fig. 5) [$P = 0.014$ using a permutation test (*18*); the maximum-likelihood estimate of λ, an index of phylogenetic dependence (*24*), for within-family extinction rate is 0.84, a value within the range typically found for ecological and morphological traits (*24*) and significantly different from zero, $P < 0.0004$; see (*18*)]. The phylogenetic signal remains significant ($P = 0.049$) under an alternative model of character change (*18*). Thus, the taxonomic and phylogenetic analyses together suggest that extinction rates in bivalves are conserved at multiple levels of evolutionary divergence, within individual families as well as among related families.

Stratigraphic ranges of taxa can be distorted by preservational and sampling biases (*17*). Our analyses hinged on differences between clades rather than differences between temporal bins, so the primary concern is not temporal variation in the quality of the fossil record (*25*, *26*), but systematic differences in preservation potential across bivalve lineages. Extinction-rate estimates are robust to differences in shell composition (*16*), but other variables known to influence preservation, such as shell size, thickness, and preferred habitats, may be important (*17*). To evaluate the robustness of our results to preservational biases, we repeated all analyses after omitting families identified by Valentine *et al.* (*17*) as having low

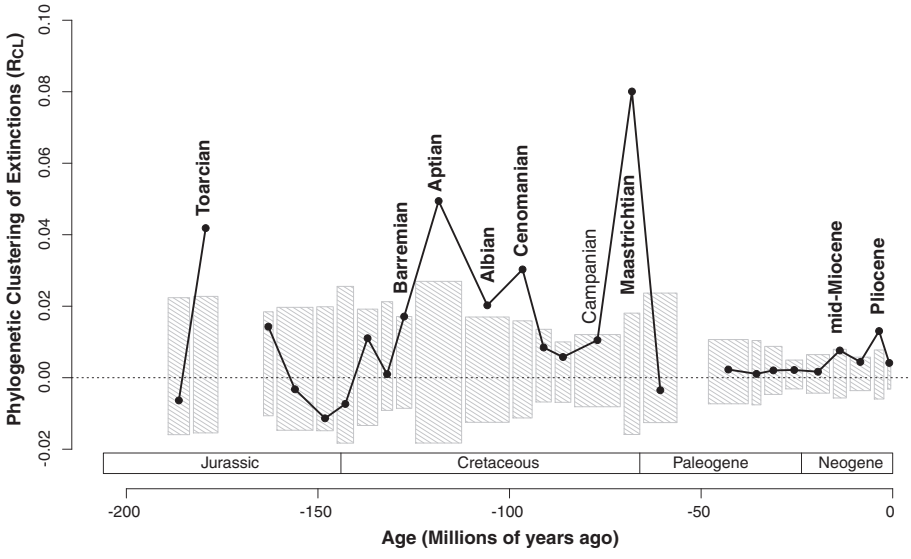

Fig. 1. Temporal trend in phylogenetic clustering of extinctions (R_{CL}). Shaded bars represent 95% confidence intervals around the expected value of R_{CL} (*18*). The intervals showing statistically significant phylogenetic clustering of extinctions are labeled in bold; an additional interval, the Campanian, is marginally significant. Only intervals with enough extinctions to analyze (eight or more) are plotted. The dotted line indicates the value expected if extinctions were not phylogenetically clustered.

preservation potential. The results were qualitatively unchanged (fig. S2). Another potential concern is that the observed differences in extinction rates between the Mesozoic and Cenozoic reflect taxonomic oversplitting of some Cretaceous groups relative to others. However, the families with disproportionate extinction represent a large and ecologically diverse assemblage (table S2), and multiple lines of evidence (*18*) suggest that the Mesozoic-Cenozoic difference is unlikely to simply reflect taxonomic practices. Phylogenetic clustering also does not appear to be driven only by extinctions associated with major environmental changes. For example, the overall signal remains highly significant, even when the Toarcian, Aptian, and Cenomanian stages, all of which include oceanic anoxic events (*27*), are excluded from the analysis, along with the Maastrichtian mass extinction (17 out of 22 extinctions with $R_{CL} > 0$, $P = 0.017$, exact binomial test).

Taken together, our results show that extinction rates of marine bivalve genera tend to be phylogenetically conserved, but the strength of this effect varies over time and can be substantially and permanently changed by a mass extinction. Lineage-level clustering of extinction rates, as seen here, is expected to follow from phylogenetic conservatism of traits that correlate with extinction vulnerability (*28*), making some lineages more prone to extinction than others (*2*, *9*, *10*). As extinction-prone taxa are winnowed out, both the rate of extinction and the associated phylogenetic clustering are expected to decrease. The stronger phylogenetic clustering seen for the Cretaceous extinctions is likely to reflect the prominence during this time of clades with volatile dynamics (table S2). The demise of these high-rate taxa at the end of the Cretaceous shifted the overall distribution to lower values and also reduced the range of variation of within-family extinction rates (Fig. 4). Such hardening of the biota over evolutionary time has been hypothesized before (*29*–*31*). Though we cannot reject the alternative hypothesis that the decline in extinction rates from Mesozoic to Cenozoic is due to a systematic decrease in extinction forcing mechanisms, we see no reason to assume that forcing mechanisms became less intense, especially given that the Cenozoic is characterized by dramatic shifts in climate, occurring on multiple temporal scales (*32*). The Mesozoic-Cenozoic differences also do not reflect differences in statistical power, because each of these eras has similar average numbers of extinctions per time interval (table S1).

Other factors such as the nature of the extinction mechanism can also contribute to the observed variations in phylogenetic clustering. Different kinds of environmental stresses are likely to cause extinctions that are selective with respect to different traits, and we might expect phylogenetic clustering of extinctions to track, in part, the degree to which the relevant traits are conserved over phylogeny. Extinction triggers that disproportionately affect specific regions or environments might also contribute to clustered extinctions in families with restricted distributions. However, virtually all bivalve families are geographically and environmentally widespread (*33*), and such spatial effects are weak in the end-Cretaceous extinction (*5*, *6*). Information on environmental drivers of past extinctions and their spatial heterogeneity is currently insufficient to permit more detailed exploration of these factors. Irrespective of the underlying causes, the influence of previous extinctions on both the magnitude of extinction rates and the pattern of phylogenetic conservatism suggests that attempts to understand the biological basis for differential extinction vulnerabilities of clades should take into account their past history of extinctions. These results also corroborate a peculiarity of the end-Cretaceous mass extinction (and perhaps of major extinctions in general), where the phylogenetic pattern of extinction is consistent with preceding intervals, as shown here, but the functional or ecological selectivity is not (*5*, *29*, *34*).

Phylogenetic nonrandomness and the temporal decline in extinction rates documented here are potentially problematic for calculating speciation and diversification rates from molecular phylogenies because they violate the assumption that extinction rates are stochastically constant over time (*35*, *36*), although recent work has started to

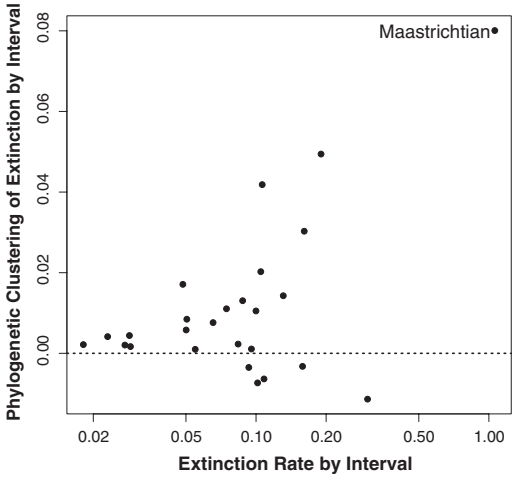

Fig. 2. Phylogenetic clustering of extinctions (R_{CL}) as a function of extinction rate, for each time interval in Fig. 1. The relation is not significant. The dotted line indicates the value expected if extinctions were not phylogenetically clustered.

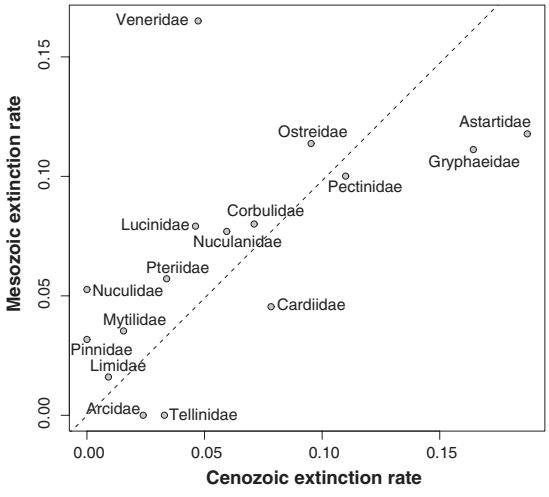

Fig. 3. Mesozoic versus Cenozoic background extinction rates for families well represented in both intervals. The dashed line represents equality in rates between the two eras ($y = x$).

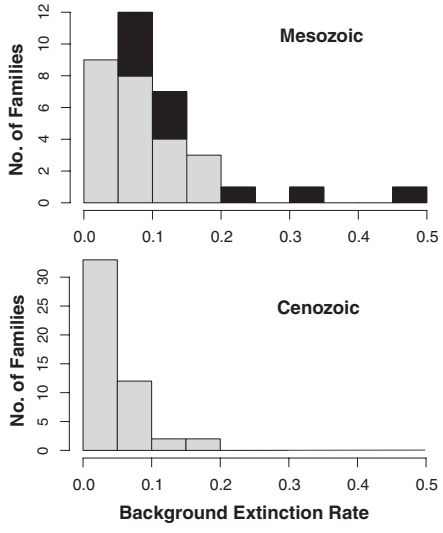

Fig. 4. Distribution of background extinction rates by family during the Mesozoic and Cenozoic eras. Black bars indicate families that went extinct during the end-Cretaceous mass extinction; gray bars indicate surviving families.

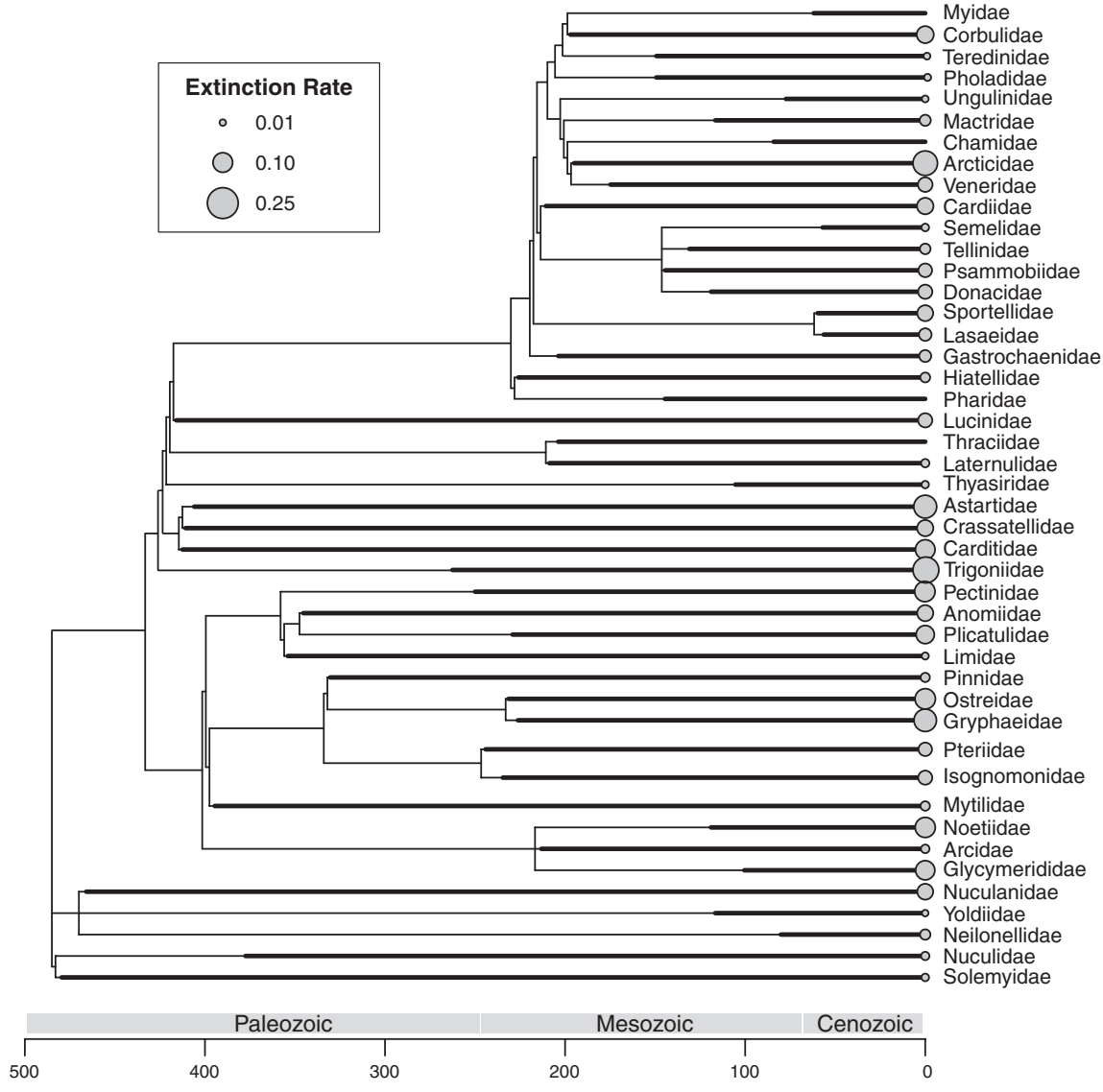

Fig. 5. Mean extinction rates for living families of bivalves mapped on the composite phylogeny used in this study (*18*). Only families for which background extinction rates could be reliably estimated (*18*) are shown. The dark bar along each branch denotes the known stratigraphic range of that taxon, omitting extinct stem groups. The size of the symbol for each family is proportional to its extinction rate. Extinction rates of closely related families are significantly more similar to each other than is expected by chance.

consider less restrictive models (*37*, *38*). On the other hand, if lineages or biotas tend to harden over time, perhaps through the filter of mass extinctions, then the assumption of stochastically constant extinction rates may be more reasonable for later histories of lineages once the more volatile taxa have been winnowed. Caution is needed, however, because such hardening might operate at multiple levels, ranging from the well-documented decline in background extinction rates through the Phanerozoic attributed to the culling of the more volatile Paleozoic fauna in favor of the more resistant Modern fauna (*39*, *40*) to the species-level selectivities seen during the marine extinction pulse near the onset of Pleistocene glacial cycles (*41*). Finally, our results combined with previous studies (*9*, *12*, *14*, *28*) imply that evolutionary histories of individual lineages are important determinants of extinction vulnerabilities of their constituent taxa, under both natural and anthropogenic forcing. This commonality suggests that more detailed studies of phylogenetic selectivity of extinctions in the geological past, and the traits involved, should provide useful insights about the consequences of extinctions unfolding today. For example, if phylogenetic clustering is a general rule, then anthropogenic extinctions are likely to eliminate substantially more evolutionary history in the near future than models based on random extinctions of the same intensity would predict (*15*).

References and Notes

1. D. Jablonski, *Philos. Trans. R. Soc. London Ser. B* **344**, 11 (1994).
2. M. L. McKinney, *Annu. Rev. Ecol. Syst.* **28**, 495 (1997).
3. D. M. Raup, *Extinction. Bad Genes or Bad Luck?* (Norton, New York, 1991).
4. S. C. Wang, A. M. Bush, *Paleobiology* **34**, 434 (2008).
5. D. Jablonski, *Paleobiology* **31** (suppl.), 192 (2005).
6. D. Jablonski, *Proc. Natl. Acad. Sci. U.S.A.* **105**, 11528 (2008).
7. J. L. Payne, S. Finnegan, *Proc. Natl. Acad. Sci. U.S.A.* **104**, 10506 (2007).
8. M. G. Powell, *Paleobiology* **33**, 530 (2007).
9. P. M. Bennett, I. P. F. Owens, D. Nussey, S. T. Garnett, G. M. Crowley, in *Phylogeny and Conservation*, A. Purvis, J. L. Gittleman, T. Brooks, Eds. (Cambridge Univ. Press, Cambridge, 2005), pp. 317–336.
10. A. Purvis, M. Cardillo, R. Grenyer, B. Collen, in *Phylogeny and Conservation*, A. Purvis, J. L. Gittleman, T. Brooks, Eds. (Cambridge Univ. Press, Cambridge, 2005), pp. 295–316.
11. G. J. Russell, T. M. Brooks, M. M. McKinney, C. G. Anderson, *Conserv. Biol.* **12**, 1365 (1998).
12. J. L. Lockwood *et al.*, *Conserv. Biol.* **16**, 1137 (2002).
13. A. Purvis, P.-M. Agapow, J. L. Gittleman, G. M. Mace, *Science* **288**, 328 (2000).
14. J. Bielby, A. A. Cunningham, A. Purvis, *Anim. Conserv.* **9**, 135 (2006).
15. A. Purvis, *Annu. Rev. Ecol. Evol. Syst.* **39**, 301 (2008).
16. S. M. Kidwell, *Science* **307**, 914 (2005).

17. J. W. Valentine, D. Jablonski, S. M. Kidwell, K. Roy, *Proc. Natl. Acad. Sci. U.S.A.* **103**, 6599 (2006).
18. Materials and Methods are available as supporting material on *Science* Online.
19. D. Jablonski, K. Roy, J. W. Valentine, *Science* **314**, 102 (2006).
20. J. J. Sepkoski, *Philos. Trans. R. Soc. London Ser. B* **353**, 315 (1998).
21. D. Jablonski, J. A. Finarelli, *Proc. Natl. Acad. Sci. U.S.A.* **106**, 8262 (2009).
22. D. Jablonski, K. Roy, J. W. Valentine, R. M. Price, P. S. Anderson, *Science* **300**, 1133 (2003).
23. J. D. Taylor, S. T. Williams, E. A. Glover, P. Dyal, *Zool. Scr.* **36**, 587 (2007).
24. R. P. Freckleton, P. H. Harvey, M. Pagel, *Am. Nat.* **160**, 712 (2002).
25. S. E. Peters, *Proc. Natl. Acad. Sci. U.S.A.* **102**, 12326 (2005).
26. A. B. Smith, A. J. McGowan, *Palaeontology* **50**, 765 (2007).
27. R. D. Pancost *et al.*, *J. Geol. Soc. London* **161**, 353 (2004).
28. M. L. McKinney, *Paleobiology* **21**, 300 (1995).
29. D. Jablonski, *Proc. Natl. Acad. Sci. U.S.A.* **98**, 5393 (2001).
30. J. B. C. Jackson, in *Extinction Rates*, J. H. Lawton, R. M. May, Eds. (Oxford Univ. Press, Oxford, 1995), pp. 45–54.
31. S. M. Stanley, *Paleobiology* **16**, 401 (1990).
32. J. Zachos, M. Pagani, L. Sloan, E. Thomas, K. Billups, *Science* **292**, 686 (2001).
33. J. A. Crame, *Paleobiology* **26**, 188 (2000).
34. S. M. Stanley, *Paleobiology* **33** (suppl.), 1 (2007).
35. S. Nee, *Annu. Rev. Ecol. Syst.* **37**, 1 (2006).
36. S. Nee, E. C. Holmes, R. M. May, P. H. Harvey, *Philos. Trans. R. Soc. London Ser. B* **344**, 77 (1994).
37. D. L. Rabosky, I. J. Lovette, *Proc. R. Soc. London Ser. B. Biol. Sci.* **275**, 2363 (2008).
38. D. L. Rabosky, I. J. Lovette, *Evolution* **62**, 1866 (2008).
39. J. J. Sepkoski Jr., in *Global Events and Event Stratigraphy*, O. H. Walliser, Ed. (Springer, Berlin, 1996), pp. 35–51.
40. J. W. Valentine, in *Causes of Evolution: A Paleontological Perspective*, R. M. Ross, W. D. Allmon, Eds. (Univ. of Chicago Press, Chicago, 1990), pp. 128–150.
41. J. T. Smith, K. Roy, *Paleobiology* **32**, 408 (2006).
42. We thank S. M. Kidwell and J. W. Valentine for discussions, I. Tëmkin and T. R. Waller for taxonomic advice, and two anonymous reviewers for insightful comments. This work was supported by a grant from NASA.

Supporting Online Material
www.sciencemag.org/cgi/content/full/325/5941/733/DC1
Materials and Methods
SOM Text
Figs. S1 to S5
Tables S1 and S2
References

4 March 2009; accepted 19 June 2009
10.1126/science.1173073

Genetic Properties of the Maize Nested Association Mapping Population

Michael D. McMullen,[1,2]‖ Stephen Kresovich,[3]‖ Hector Sanchez Villeda,[2]* Peter Bradbury,[1,3] Huihui Li,[4,5,3] Qi Sun,[6] Sherry Flint-Garcia,[1,2] Jeffry Thornsberry,[7] Charlotte Acharya,[3] Christopher Bottoms,[2] Patrick Brown,[3] Chris Browne,[1] Magen Eller,[1] Kate Guill,[1] Carlos Harjes,[3]† Dallas Kroon,[3] Nick Lepak,[1] Sharon E. Mitchell,[3] Brooke Peterson,[1] Gael Pressoir,[3]‡ Susan Romero,[1] Marco Oropeza Rosas,[8]¶ Stella Salvo,[1] Heather Yates,[3] Mark Hanson,[9] Elizabeth Jones,[10] Stephen Smith,[10] Jeffrey C. Glaubitz,[11] Major Goodman,[8] Doreen Ware,[1,12] James B. Holland,[1,8]‖ Edward S. Buckler[1,3,13]‖

Maize genetic diversity has been used to understand the molecular basis of phenotypic variation and to improve agricultural efficiency and sustainability. We crossed 25 diverse inbred maize lines to the B73 reference line, capturing a total of 136,000 recombination events. Variation for recombination frequencies was observed among families, influenced by local (cis) genetic variation. We identified evidence for numerous minor single-locus effects but little two-locus linkage disequilibrium or segregation distortion, which indicated a limited role for genes with large effects and epistatic interactions on fitness. We observed excess residual heterozygosity in pericentromeric regions, which suggested that selection in inbred lines has been less efficient in these regions because of reduced recombination frequency. This implies that pericentromeric regions may contribute disproportionally to heterosis.

The majority of phenotypic variation in natural populations and agricultural plants and animals is determined by quantitative genetic traits (*1*). Maize (*Zea mays* L.) exhibits extensive molecular and phenotypic variation (*2*–*4*). Understanding the genetic basis of quantitative traits in maize is essential to predictive crop improvement. However, only slow progress has been made in identifying the genes controlling quantitative agronomic traits because of limitations in the scope of allelic diversity and resolution in available genetic mapping resources. Linkage mapping generally focuses on the construction and analysis of large families from two inbred lines to detect quantitative trait loci (QTLs) (*5*). However, resolution of these QTLs can be poor because of the limited number of recombination events that occur during population development. Association analysis takes advantage of historic recombination from deep coalescent history as linkage disequilibrium (LD) generally decays within 2 kb (*1*, *6*). However, because of the number of single-nucleotide polymorphisms (SNPs) required and the confounding effects of population structure, whole-genome association analysis can be difficult in maize (*4*).

To provide a genetic resource for quantitative trait analysis in maize, we have created the nested association mapping (NAM) population. NAM was constructed to enable high power and high resolution through joint linkage-association analysis, by capturing the best features of previous approaches (*7*, *8*). The genetic structure of the NAM population is a reference design of 25 families of 200 recombinant inbred lines (RILs) per family (fig. S1). The inbred B73 was chosen as the reference inbred line because of its use for the public physical map (*9*) and for the Maize Sequencing Project (www.maizesequence.org). The other 25 parents [named the 25 diverse lines (25DL)] maximize the genetic diversity of the RIL families (*8*, *10*), independent of any specific phenotype. The lines were chosen to represent the diversity of maize—more than half are tropical in origin, nine are temperate lines, two are sweet corn lines (representing Northern Flint), and one is a popcorn inbred line (fig. S2).

The NAM genetic map is a composite map created with 4699 RILs combined across the 25 families, representing 1106 loci, with an average marker density of one marker every 1.3 centimorgans (cM) (fig. S3 and table S1). The proportion of SNP loci from the composite map polymorphic in an individual family ranged from 63 to 74%. Among RILs, 48.7% of all marker genotypes were inherited from B73, 47.6% were inherited from the 25DL parent, and 3.6% were heterozygous, which suggests that they were broadly representative of the parents and fall within the expected range for S5 generation RILs. The NAM population captured ~136,000 crossover events, corresponding, on average, to three crossover events per gene. This allows genetic factors to be mapped to very specific regions of the

[1]United States Department of Agriculture–Agriculture Research Service (USDA–ARS). [2]Division of Plant Sciences, University of Missouri, Columbia, MO 65211, USA. [3]Institute for Genomic Diversity, Cornell University, Ithaca, NY 14853, USA. [4]School of Mathematical Science, Beijing Normal University, Beijing 100875, China. [5]Institute of Crop Science, Chinese Academy of Agricultural Sciences, Beijing 100081, China. [6]Computational Biology Service Unit, Cornell University, Ithaca, NY 14853, USA. [7]Northwest Missouri State University, Maryville, MO 64468, USA. [8]Department of Crop Science, North Carolina State University, Raleigh, NC 27695, USA. [9]Illumina Inc., San Diego, CA 92121, USA. [10]Pioneer Hi-Bred, Johnston, IA 50131, USA. [11]Laboratory of Genetics, University of Wisconsin, Madison, WI 53706, USA. [12]Cold Spring Harbor Laboratory, Cold Spring Harbor, NY 11724, USA. [13]Department of Plant Breeding and Genetics, Cornell University, Ithaca, NY 14853, USA.

*Present address: International Maize and Wheat Improvement Center (CIMMYT), kilometer 45, Carretera Mex-Veracruz, El Batan, Texcoco, Mexico.
†Present address: Monsanto, Leesburg, GA 31763, USA.
‡Present address: Fondation CHIBAS, 30 Rue Pacot, Port-au-Prince, Haiti.
¶Present address: Delta Pine/Monsanto, Post Office Box 194, Scott, MS 38772, USA.
‖To whom correspondence should be addressed. E-mail: mcmullenm@missouri.edu (M.D.M.); sk20@cornell.edu (S.K.); james_holland@ncsu.edu (J.B.H.); esb33@cornell.edu (E.S.B.)

Supporting Online Material for

Phylogenetic Conservatism of Extinctions in Marine Bivalves

Kaustuv Roy,* Gene Hunt, David Jablonski

*To whom correspondence should be addressed. E-mail: kroy@ucsd.edu

Published 7 August 2009, *Science* **325**, 733 (2009)
DOI: 10.1126/science.1173073

This PDF file includes:

Supporting Online Material

Materials and Methods

Data: We used an updated version of the database of Jablonski et al. (*S1*) to calculate extinction rates of marine bivalve genera. This database consists of stratigraphic ranges of bivalve genera and subgenera [hereafter termed genera since they are commonly considered to be of equivalent rank; (*S1*)] with a known fossil record. The data were taxonomically standardized using the molluscan taxonomic literature, museum collections and consultation with molluscan systematists (*S2*). Stratigraphic ranges were placed into a standard time scale of 33 intervals from the beginning of the Jurassic to the Pleistocene (Table S1). These intervals correspond to stages in the Mesozoic (or rarely, combinations of two relatively short stages) and sub-epochs in the Cenozoic (mean duration = 6.24 Million years [Myr], standard deviation = 3.0 Myr). Genera whose first or last occurrences could not be resolved to these intervals, or were uncertain, were excluded from the analysis. A total of 1678 genera were used for the analyses presented here.

Calculation of extinction rates: We computed extinction rates using the boundary-crossers method, which has better statistical properties than other metrics that can be calculated using stratigraphic ranges (*S3*). With this approach, extinction rate (q) for an interval is calculated as $q = -\ln(N_{bt} / N_b) / \Delta t$, where N_b is the number of taxa that cross the interval's lower boundary, N_{bt} is the number of taxa that cross its lower and upper boundary, and Δt is the duration of the interval (*S3*). We calculated the extinction rates on a per-interval basis, rather than per million years ($\Delta t = 1$ for all intervals). This approach is preferred given the generally pulsed rather than continuous nature of

extinction the marine fossil record (*S4*), but for our purposes it makes little difference whether the rates are calculated as per-interval or per-million-year rates since the two metrics are very highly correlated (Spearman rank correlation, $r_s = 0.79$, $P < 1 \times 10^{-6}$, $n =$ 32 intervals). The rate metric used here ignores taxa restricted to a single stratigraphic interval ("singletons"), as it has been shown that the ranges of these taxa can be highly influenced by incompleteness of the fossil record (*S3*). Per-interval extinction rates for all analyzed intervals are shown in Table S1.

Extinction clustering: We computed an index of phylogenetic clustering separately for each time interval used here. The index of clustering R_{CL} is defined as the matrix correlation between two matrices, M_{TAX} and M_{EXT}. Each matrix represents the pairwise association of all genera entering the interval in question (i.e., crossing the bottom boundary). M_{TAX} represents the taxonomic similarity between genera; it takes values of 1 for genera in the same family, and 0 for genera in different families. M_{EXT} represents extinction similarity; it takes on a value of 1 when the two genera jointly go extinct and 0 otherwise. R_{CL} values will be high when the genera going extinct are preferentially drawn from a few families and lower when the extinct genera are distributed more evenly across families (i.e. no phylogenetic clustering of extinctions). Hypothetical examples of the M_{TAX} and M_{EXT} matrices, and of the calculation of R_{CL}, are shown in Figure S1.

We calculated the null distribution of R_{CL} separately for each interval by simulating extinction that is random with respect to family membership. If an interval had x extinctions, x genera were chosen at random from all those entering the interval (N_b) and declared extinct. This was repeated 5,000 times, with R_{CL} calculated each time. The distribution of R_{CL} for the simulated data forms the null distribution of the statistic. The

mean of the null distribution for R_{CL} is very close to zero in each interval, and thus this metric provides a useful index for comparing the pattern of clustering over time; because the distribution is skewed, the confidence intervals for R_{CL} are somewhat asymmetrical. The metric R_{CL} is similar to Moran's *I*, which has previously been used to investigate taxonomic clustering of extinctions (*S5*); in fact, the matrix M_{TAX} is equivalent to the weighting matrix used in the computation of Moran's *I*. Following (*S5*) we also computed the Moran's *I* statistic as a measure of extinction clustering. For our data Moran's *I* appears to be somewhat sensitive to the number of taxa (N_b) and possibly the number of extinctions (the mean *I* value for simulated random extinction is high in the Jurassic, and converges on zero as N_b increases towards the Recent). Nevertheless, Moran's *I* and R_{CL} are in exact agreement as to which intervals show significant extinction clustering by families.

While we provide the estimates of R_{CL} for all intervals in our dataset with 8 or more extinctions, the power to detect phylogenetic clustering in many of these is low due to few extinctions. Thus we have mainly focused on the aggregate pattern of phylogenetic clustering over the entire time-series. When analyzing the time-series of extinctions, we have not adjusted the p-values of individual events for multiple comparisons. As far as the overall trend of extinction clustering is concerned, if extinctions are random with respect to family membership, the R_{CL} statistic is equally likely to take on positive and negative values. However, results of binomial tests (see main text and below) suggest that it is highly unlikely that so many intervals would show positive values of R_{CL} in the absence of real clustering. Second, although sequential Bonferroni correction is often used to adjust the p-values of multiple comparisons, mathematical and logical concerns

about the use of this method have been raised (*S6*). In analyses such as ours the use of sequential Bonferroni correction would greatly inflate the type II error and thus make the tests overly conservative (see *S6*). A single significant p-value in a large set of comparisons should indeed be treated with caution, but many significant values suggest that a biologically real signal is present (*S6*). In our case the highly significant binomial tests confirms this. Finally, we note that even when a sequential Bonferroni correction is applied, significant extinction clustering is still evident for three of the time intervals.

Tree-based Clustering among Families: The preceding analyses test whether genus extinctions are clustered within families. We next tested for the presence of phylogenetic signal in extinction rates at the deeper nodes of the bivalve phylogenetic tree, specifically for extinction rates calculated separately by family. Such a test requires three components: (i) within-family extinction rates, (ii) a phylogenetic hypothesis among bivalve families, and (iii) a statistical test for phylogenetic signal.

Extinction rates were computed separately for each family using the boundary-crosser method described above. We restricted these computations to background extinction intervals, but including the Maastrichtian Stage (the only major mass extinction interval in our analyses) has little effect on overall extinction rates (Spearman rank correlation $r_s = 0.94$ between extinction rates when including versus excluding the Maastrichtian). In addition, we limited the analysis to families with at least 30 lower boundary crossings (N_b) so as to eliminate poorly estimated extinction rates.

For our phylogenetic hypothesis, we used a composite molecular phylogeny using the tree from Giribet and Distel (*S7, Fig. 3.6*) as the starting point and modifying it to reflect the results of subsequent studies by Taylor et al. (*S8, Fig. 2*, for the relationships among

the heterodonts), Bieler and Mikkelsen (*S9*) and Giribet (*S10*). Following Waller (*S11-13*), we shifted the calcitic taxa traditionally placed in the Malleidae to the extinct family Eligmidae, which is evidently more closely related to Ostreoidea than to Pterioidea; this taxonomic and phylogenetic re-assignment drops the Malleidae below our sample size threshold for inclusion. The stratigraphic ranges of families were used to determine branch lengths of this tree, with each node and tip dated to the age of its oldest included taxon.

To test for phylogenetic signal, we used a non-parametric test built around the computation of phylogenetically independent contrasts (*S14*). The set of contrasts represent differences in trait value—here, extinction rate—between taxa and nodes that are chosen to span all branches of the tree exactly once (*S15*). We compared the observed variance of the contrasts to a null distribution computed after randomly permuting the taxon labels from the tree a 1000 times. This permutation retains the same distribution of extinction rates and phylogenetic relationships as the original data, but destroys any phylogenetic coherence in the rates. If extinction rates show substantial phylogenetic signal, closely related taxa will have similar rates and the observed variance of the contrasts will be much lower than the variance of the contrasts in the permuted data. This test was treated as one-tailed (see *S14*), and so the P-value is simply the proportion of null replicates with contrast variances lower than the observed value.

There were two methodological issues in executing this test. First, extinction rates among families are highly right-skewed, which causes the few highest rates to dominate the calculation of the variance of the contrasts. In order to lessen the effect of these outlying extinction rates, we square-root-transformed extinction rates prior to

analysis. The second issue here stems from the fact that the phylogenetic relationships are not fully resolved, which causes ambiguities in defining the independent contrasts. We addressed this problem by resolving polytomies randomly to create a fully bifurcating tree. To explore the effects of difference possible resolution of polytomies, we repeated the analysis with 100 different random resolutions of polytomies, performing 1,000 permutations for each resolution. The reported P-value ($P = 0.014$) is the average over these 100 iterations, all of which fall within a narrow range (between 0.004 and 0.027).

In addition to this randomization approach, we also tested for phylogenetic signal using the model-based method from Freckleton et al. (*S16*). This approach tests for phylogenetic signal by estimating a tree-transformation parameter (λ). When $\lambda=0$, trees become a star phylogeny, which is indicative of no phylogenetic signal for the trait in question. A value of $\lambda=1$ is consistent with Brownian motion trait evolution and high phylogenetic signal. The maximum-likelihood estimate of λ for within-family extinction rate, square-root transformed, is 0.84. This value is within the range typically found for ecological traits (*S16*) and is significantly different from zero (likelihood ratio test statistic = 12.52, $P = 0.0004$, comparing the model with $\lambda=0.84$ to a model in which $\lambda=0$). This test is unaffected by polytomies, and so it was not necessary to randomly resolve unresolved nodes. Finally, we used an alternative approach to explore whether our result is sensitive to the model of character change [gradual versus punctuational (*S17*)] by calculating the maximum likelihood estimate of the scaling parameter Kappa (*S17*) for our tree, and repeating the permutation test after transforming the phylogeny using this estimate (Kappa = 0.40). The signal remained significant (P = 0.049).

Is the Mesozoic-Cenozoic difference in rates due to taxonomic practice? We evaluated this issue using multiple proxies because directly quantifying variations in taxonomic practices is extremely difficult, if not impossible. First, if extinction rates are related to the degree of taxonomic splitting, then more finely divided groups, in our case those with fewer species per genus, should also show higher extinctions. Because reliable estimates of species richness of individual genera are lacking for most of the intervals used in this study except for the Maastrichtian (*S18*), we used the latter as a proxy for the other Mesozoic intervals used here. As figure S3 shows, there is no significant correlation ($P = 0.45$, Spearman Rank correlation) between the median species/genus ratio for each family and its background extinction rate during the Mesozoic (i.e., excluding the end-Cretaceous extinction). This indicates that families with high extinction rates do not necessarily have few species per genus; inoceramids, ostreids and a few other families have relatively high genus extinction despite having species-rich genera. Note that this test assumes that all differences in species/genus ratios reflect taxonomic practice and not biology, so our results are conservative. Furthermore, for the end-Cretaceous extinction, previous multivariate analyses (*S18*) found that species richness does not directly affect genus survivorship but geographic range is a major factor (multiple logistic regression predicting genus survivorship: $P = 0.85$ for species richness, and $P = 0.002$ for geographic range measured by number of biogeographic provinces occupied).

Next we tested whether the differences are driven by rudists and inoceramids, two Mesozoic groups used for biostratigraphy and hence potentially more finely subdivided than others. As Figure S4 shows, when both rudists and inoceramids are excluded from the analyses, the levels of clustering for the individual Mesozoic intervals are affected

(e.g. the Maastrichtian is less of an outlier) but the overall pattern of phylogenetic clustering remains qualitatively the same. Changes in specific intervals are to be expected since these two families are important components of Mesozoic bivalve diversity.

Finally, we also calculated extinction rates and the temporal pattern of clustering after including single interval taxa, which are commonly excluded from analyses of extinction rates due to taxonomic and preservational concerns. Again, their inclusion changes the values for some of the intervals, as would be expected, but the overall trend remains qualitatively the same (Fig. S5). Taken together these tests strongly suggest that the overall trends in extinction rates and the patterns of phylogenetic clustering reported here are unlikely to be simply artifacts of taxonomic practices.

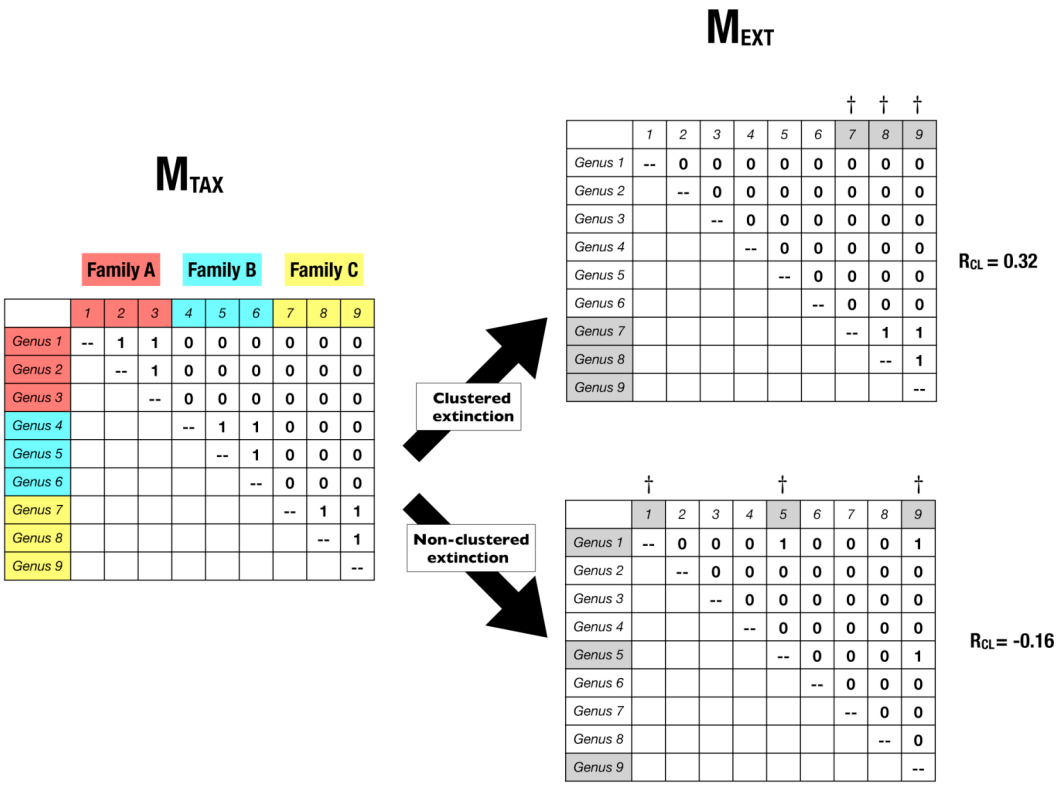

Figure S1. Hypothetical example showing the calculations of extinction clustering. On the left, the M_{TAX} matrix represents the association of genera into families. Each pair of genera receives a score: 1 for genera from the same family, and 0 for genera from different families. Shown here are nine genera from three different families (family A in red, family B in blue, and family C in yellow). On the right are two different extinction matrices (M_{EXT}), one with extinctions clustered in family C (top), the other with extinctions distributed in each of the three families (bottom). Grey shading and dagger symbols indicate genera that go extinct (genera 7, 8 and 9 in the top matrix, genera 1, 5 and 9 in the bottom). Entries in the M_{EXT} matrix are 1 for pairs of genera that both go extinct, and 0 otherwise. The test statistic, R_{CL}, is simply the matrix correlation between corresponding elements of the M_{TAX} and M_{EXT} matrices.

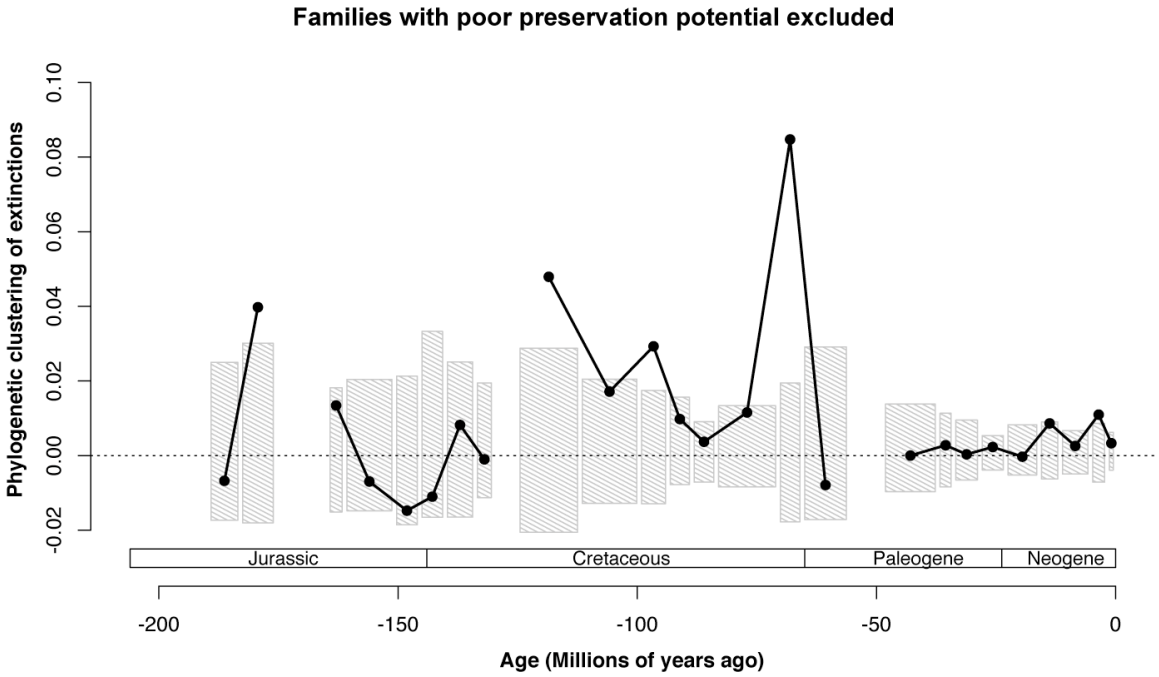

Figure S2. Temporal trend in phylogenetic clustering of extinctions (R_{CL}) after excluding families with low preservation potential (following *17*). The shaded bars represent 95% confidence intervals around the expected value of R_{CL}.

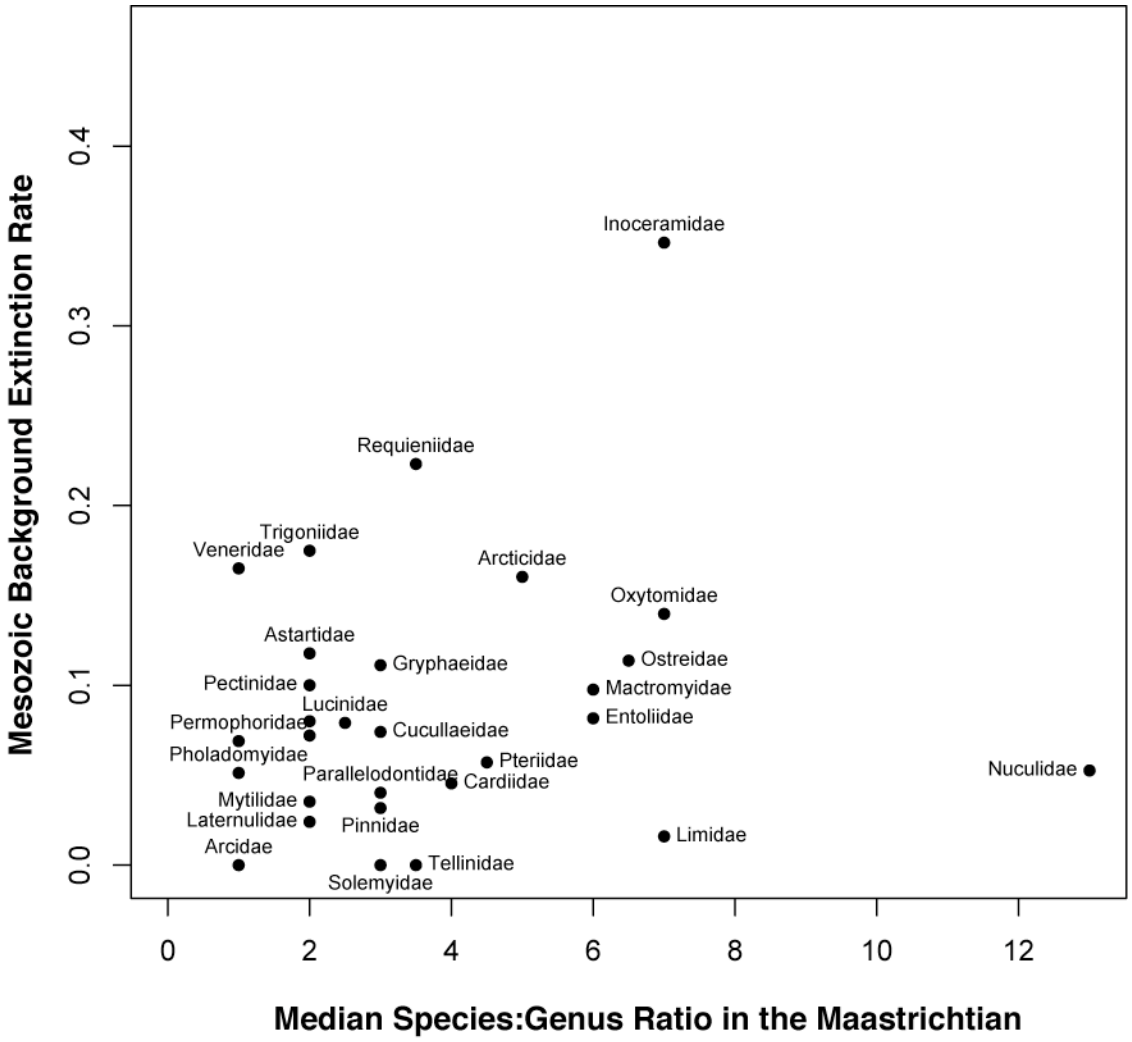

Figure S3. Relationship between the median species/genus ratio of families during the Maastrichtian and their background extinction rates over the Mesozoic intervals used in this study (only families for which background extinction rates could be reliably estimated, N_b>=30, are shown; see text for details).

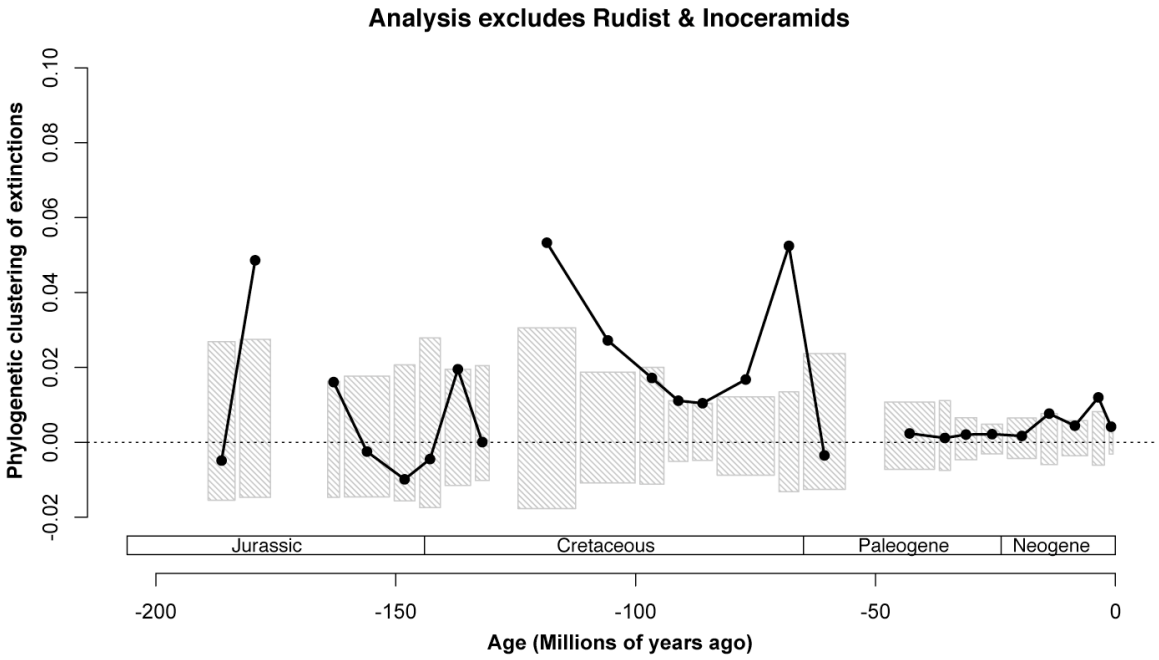

Figure S4. Temporal trend in phylogenetic clustering of extinctions (R_{CL}) when all genera of rudists and inoceramids are excluded from the analysis (see text for details). The shaded bars represent 95% confidence intervals around the expected value of R_{CL}.

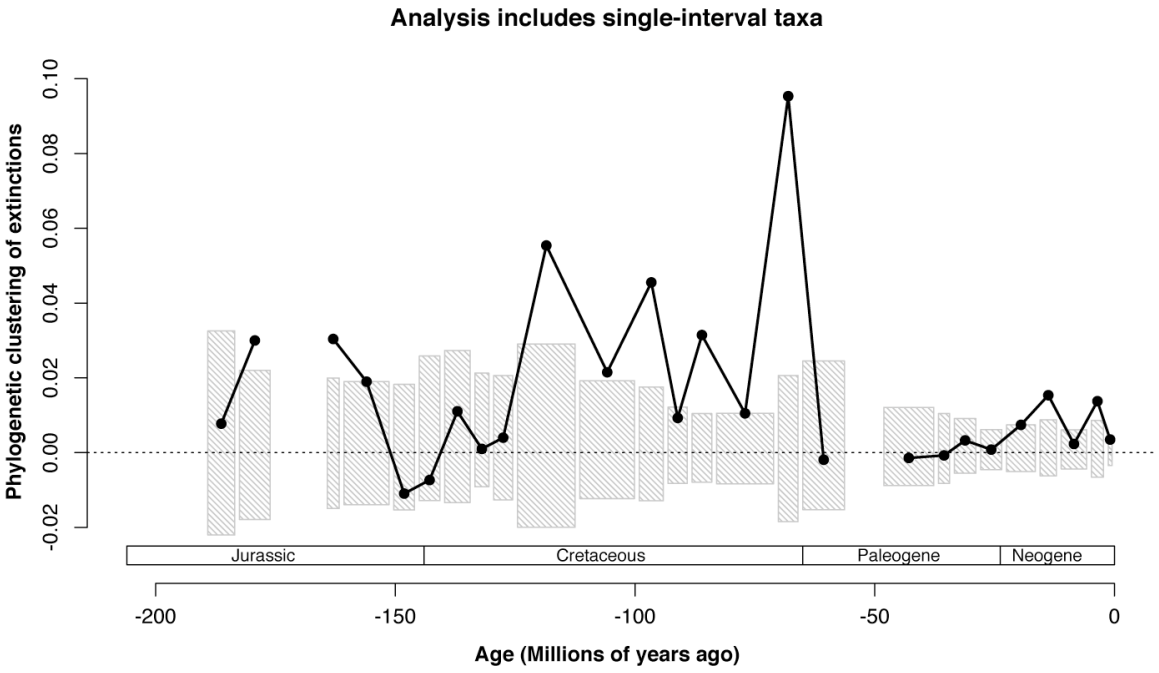

Figure S5. Temporal trend in phylogenetic clustering of extinctions (R_{CL}) when single-interval genera ("singletons") are included (see text for details). The shaded bars represent 95% confidence intervals around the expected value of R_{CL}.

Table S1. Geological intervals and associated extinction rate estimates. Ages, in millions of years before present, indicate the start (base) of each interval (*S19*). Also shown for each interval are the number of genera crossing that interval's lower boundary (N_b), the number of the lower boundary crossers that go extinct during the interval ($N_e = N_b - N_{bt}$). Note that rates cannot be computed for the first and last intervals using the boundary crossing method.

No.	Interval	Age	N_b	N_e	Extinction rate
1	pre-Jurassic	>206	--	--	--
2	Hettangian	199.6	78	1	0.013
3	Sinemurian	196.5	108	3	0.028
4	Pliensbachian	189.6	117	12	0.108
5	Toarcian	183	119	12	0.106
6	Aalenian	175.6	123	1	0.008
7	Bajocian	171.6	134	5	0.038
8	Bathonian	167.7	155	6	0.039
9	Callovian	164.7	163	20	0.131
10	Oxfordian + Kimmeridgian	161.2	157	23	0.158
11	Tithonian	150.8	173	45	0.301
12	Berriasian	145.5	145	14	0.102
13	Valanginian	140.2	139	10	0.075
14	Hauterivian	136.4	150	8	0.055
15	Barremian	130	169	8	0.048
16	Aptian	125	179	31	0.190

17	Albian	112	201	20	0.105
18	Cenomanian	99.6	242	36	0.161
19	Turonian	93.5	244	12	0.050
20	Coniacian + Santonian	89.3	266	13	0.050
21	Campanian	83.5	305	29	0.100
22	Maastrichtian	70.6	332	217	1.060
23	Paleocene	65.5	135	12	0.093
24	Eocene - lower	55.8	264	5	0.019
25	Eocene - mid	48.6	361	29	0.084
26	Eocene - upper	37.2	439	40	0.096
27	Oligocene - lower	33.9	445	12	0.027
28	Oligocene - upper	28.4	501	9	0.018
29	Miocene - lower	23.03	562	16	0.029
30	Miocene - mid	15.97	711	45	0.065
31	Miocene - upper	11.61	745	21	0.029
32	Pliocene	5.3	787	66	0.088
33	Pleistocene	1.8	834	19	0.023
34	Recent	0	--	--	--

Table S2. The total diversity, number of extinctions (*N* and N_e, both exclude single-interval genera), those families in which extinctions are disproportionate, and their mode of life for each of the eight intervals with significant phylogenetic clustering and the Campanian, which is marginally significant. Within each interval, families with extinction proportions greater than the mean of the interval are listed in order of decreasing extinction intensity. Families of rudists are underlined. Note that in some cases, still-living families experience apparent total extinction (e.g., the Donacidae during the Maastrichtian). This can occur when the fossil record is incomplete, i.e., all known genera go extinct during an interval, but other genera range through without being sampled. Additionally, some genera known to range through extinction intervals had to be excluded from these analyses because their range endpoints were not resolved to the required stratigraphic resolution. Total diversity (*N*) here includes all genera except for those restricted to a single interval. The abbreviations for mode of life are: E = epifaunal suspension feeder, NI = non-siphonate infaunal suspension feeder SI = siphonate infaunal suspension feeder, C = commensal, S = symbiont-bearing (chemoautotrophic), CA = carnivore.

Interval	**Total *N***	**Total N_e**	**Families with Disproportionate extinction [#N_e / # *N*]**	**Mode of Life**
Toarcian	135	12	Carditidae [2/2] Cardiniidae [2/2] Trigoniidae [2/7] Pectinidae [3/12] All others [3/112]	NI NI NI E
Barremian	187	8	Trigoniidae [3/28] All others [5/159]	NI
Aptian	232	31	<u>Caprinidae</u> [5/9] Arcticidae [4/8] Cucullaeidae [2/4] <u>Requieniidae</u> [2/5] Trigoniidae [7/28] Pectinidae [2/9]	E SI NI E NI E

			All others [9/189]	
Albian	262	20	Inoceramidae [2/2] Oxytomidae [2/3] Veneridae [3/9] Trigoniidae [4/25] All others [9/223]	E E SI NI
Cenomanian	280	36	Neomiodontidae [2/2] Caprotinidae [4/6] Caprinidae [6/11] Carditidae [2/5] Trigoniidae [5/23] All others [17/233]	SI E E NI NI
Campanian	361	29	Trigoniidae [5/19] Gryphaeidae [2/9] Ostreidae [2/12] Veneridae [2/17] Radiolitidae [3/31] All others [15/273]	NI E E SI E
Maastrichtian	352	217	Trigoniidae [14/14] Requieniidae [2/2] Radiolitidae [28/28] Neitheidae [2/2] Monopleuridae [2/2] Mactromyidae [2/2] Inoceramidae [4/4] Hippuritidae [10/10] Donacidae [3/3] Dicerocardiidae [2/2] Caprinidae [7/7] Bakevelliidae [5/5] Ostreidae [10/11] Veneridae [14/15] Astartidae [6/7] Poromyidae [3/4] Laternulidae [3/4] Gryphaeidae [5/7] Cardiidae [10/14] Mactridae [6/9] Tellinidae [6/9] Tancrediidae [2/3] Pholadomyidae [4/6] Pectinidae [6/9] Parallelodontidae [4/6] Glycymerididae [2/3] Clavagellidae [2/3] Arcticidae [4/6] All others [49/155]	NI E E E E SI E E SI NI E E E SI NI CA SI E SI SI D/SI SI SI E E NI SI SI
Miocene-mid	790	45	Leptonidae [2/7] Kelliidae [2/8] Carditidae [3/25]	C C NI

			Pectinidae [6/63] Cardiidae [4/42] Veneridae [9/106] All others [18/539]	E SI SI
Pliocene	900	66	Isognomonidae [2/4] Astartidae [3/7] Glycymerididae [4/10] Leptonidae [2/5] Pectinidae [12/69] Lucinidae [5/47] Mactridae [4/39] Veneridae [11/119] Cardiidae [4/43] All others [19/557]	E NI NI C E S SI SI SI

Supporting References

S1. D. Jablonski, K. Roy, J. W. Valentine, R. M. Price, P. S. Anderson, *Science* **300**, 1133 (2003).

S2. D. Jablonski, K. Roy, J. W. Valentine, *Science* **314**, 102 (2006).

S3. M. Foote, *Paleobiology* **26**, 74 (2000).

S4. M. Foote, *Paleobiology* **31**, 6 (2005).

S5. J. L. Lockwood *et al.*, *Conserv. Biology* **16**, 1137 (2002).

S6. M. D. Moran, *Oikos* **100**, 403 (2003).

S7. G. Giribet, D. L. Distel, in *Molecular Systematics and Phylogeography of Mollusks,* C. Lydeard, D. R. Lindberg, Eds. (Smithsonian Books, Washington, 2003), pp. 45-90.

S8. J. D. Taylor, S. T. Williams, E. A. Glover, P. Dyal, *Zool. Scr.* **36**, 587 (2007).

S9. R. Bieler, P. M. Mikkelsen, *Zool. Jour. Linn. Soc.* **148**, 223 (2006).

S10. G. Giribet, in *Phylogeny and evolution of the Mollusca,* W. F. Ponder and D. R. Lindberg, Eds. (University of California Press, Berkeley, 2008), pp. 105-141.

S11. T. R. Waller, *Phil. Trans. R. Soc. London Ser B* **284**, 345 (1978).

S12. T. R. Waller, *J. Paleontol.* **59**, 768 (1985)

S13. T. R. Waller, in *Bivalves: An eon of evolution,* P. A. Johnston and J. W. Haggart, Eds. (University of Calgary Press, Calgary, 1998), pp. 1-45.

S14. S. P. Blomberg, T. Garland, A. R. Ives, *Evolution* **57**, 717 (2003).

S15. J. Felsenstein, *Amer. Nat.* **125**, 1 (1985).

S16. R. P. Freckleton, P. H. Harvey, M. Pagel, *Amer. Nat.* **160**, 712 (2002).

S17. M. Pagel, *Proc. R. Soc. London Ser. B* **255**, 37 (1994)

S18. D. Jablonski, *Proc. Natl. Acad. Sci. USA* **105**, 11528 (2008).

S19. J. G. Ogg, G. Ogg, F. M. Gradstein, *The Concise Geologic Time Scale* (Cambridge University Press, Cambridge, 2008)